The Journal of Chemical Physics

RESEARCH ARTICLE | JANUARY 30 2026

Electron scattering on carbon monoxide: An optimization of target molecular orbitals

Fan Fang ; He Su ; Jonathan Tennyson ; Qunchao Fan; Zhixiang Fan ; Hong Zhang; Xinlu Cheng

J. Chem. Phys. 164, 044309 (2026)
https://doi.org/10.1063/5.0307607

The Journal of Chemical Physics ARTICLE pubs.aip.org/aip/jcp

Electron scattering on carbon monoxide: An optimization of target molecular orbitals

Cite as: J. Chem. Phys. 164, 044309 (2026); doi: 10.1063/5.0307607
Submitted: 17 October 2025 • Accepted: 31 December 2025 •
Published Online: 30 January 2026

Fan Fang,[1] He Su,[1,a)] Jonathan Tennyson,[2] Qunchao Fan,[1] Zhixiang Fan,[1] Hong Zhang,[3] and Xinlu Cheng[4]

AFFILIATIONS

[1] School of Science, Key Laboratory of High Performance Scientific Computation, Xihua University, Chengdu 610039, China
[2] Department of Physics and Astronomy, University College London, London WC1E 6BT, United Kingdom
[3] College of Physics, Sichuan University, Chengdu 610065, China
[4] Institute of Atomic and Molecular Physics, Sichuan University, Chengdu 610065, China

[a)] **Author to whom correspondence should be addressed:** suhe@xhu.edu.cn

ABSTRACT

An accurate description of target molecular orbitals is essential for modeling the electron–molecule scattering process. Here, we devise a framework for optimizing target molecular orbitals by numbering and weighting state-averaged molecular configuration wave functions automatically according to the experimental parameters to investigate low-energy electron scattering from carbon monoxide using the *ab initio* R-matrix method. Its main feature is the ability to provide optimal target molecular orbitals in terms of various specific elastic and inelastic scattering processes. Agreement with the available measurements and previous calculations is mostly excellent. The good description of the electronic dipole moment for the CO molecule plays a key role in determining the rotational excitation and elastic scattering results. The electronic excitation energies contribute to the accuracy of electronic excitation cross sections, with a low root-mean-square error of only 0.06 Å^2. This study may pave a promising pathway for enhancing the study of electron–molecule scattering.

I. INTRODUCTION

Reliable data for electron–molecule collisions are of great importance, especially in understanding phenomena in cool plasmas and discharges. The recognition of the importance of the theoretical research field in electron scattering[1] means that improving the quality and the theoretical assessment of electron-scattering cross sections is still essential. Current theoretical and computational models for the low-energy scattering process still cannot yet rival the level of accuracy achieved by the construction of target wave functions.

Carbon monoxide is a simple polar diatomic molecule that has become a benchmark system for *ab initio* electronic structure studies.[2,3] The study of electron collisions with CO molecules aids in understanding the electron cooling process in the atmospheres of Mars and Venus, as well as molecular chemical evolutions. As one of the most popular research directions, the scattering from the CO molecule has been extensively investigated by several experimental groups; here, we mainly focus on the low-energy regions. The total scattering cross sections were measured by Kwan *et al.*[4] applying a beam-transmission technique below 500 eV. Buckman and Lohmann[5] employed a time-of-flight spectrometer technique in the energy range 0.5–5 eV. Kanik *et al.*[6] used a linear attenuation technique at 5–300 eV, and Szmytkowski *et al.*[7] used a linear transmission method at impact energies between 0.5 and 250 eV, respectively. Gibson *et al.*[8] and Tanaka *et al.*[9] reported elastic differential cross sections by using the crossed beam spectrometer technique with electron energies below 30 and 100 eV, respectively. Mason and Newell[10] reported the electronic excitation cross sections from the ground state to the $I\,^1\Sigma^-$ excited state below 60 eV. Haddad and Millory[11] determined the momentum transfer cross sections in the energy range of 1–4 eV. Recently, Alan[12] reported measurements of integral elastic cross sections and momentum transfer cross sections for the energy range 0.5–10 eV. In addition, Brunger and Buckman[13] and Itikawa[14] provided comprehensive reviews on elastic and inelastic scattering cross sections.

The very popular R-matrix methodology can formally produce a complete description of electron–molecule scattering processes

in the low energy regions,[15,16] as indicated by previous studies on the CO molecule.[17–20] Over the past few years, Dora *et al.*[21–23] investigated the effect of different Gaussian basis sets (cc-pVDZ, cc-pVTZ, and cc-pV6Z) and different active spaces employing the state-averaged complete active space self-consistent field (SA-CASSCF) method on target calculations to improve the accuracy of electron collision with CO. Their studies indicate that larger bases can detect more resonances, while their total and elastic cross section results are significantly higher than the experimental values, especially near the first peak associated with the $^2\Pi$ shape resonance. Recently, Zawadzki *et al.*[24,25] showed the electronic excitation scattering results below 30 eV with target calculations using the SA-CASSCF method with a large cc-pVQZ Gaussian basis set and involving forty-one electronic states. Very recently, Wei *et al.*[26] computed electronic excitation and de-excitation cross sections from the ground electronic state of CO using the R-matrix method with a cc-pVQZ basis set, obtaining limited improvements over previous studies. Moreover, there are few studies of electron-impact rotational excitation processes, which are challenging in the astrophysically important very low energy region; see Chandra,[27] who used Wigner–Eisenbud R-matrix calculations, and the experiments of Randell *et al.*[28] Several other theoretical methods have been used to study electron scattering from carbon monoxide in the high energy regime,[29,30] which is not addressed in the present study. The available studies do not always agree about the magnitudes of elastic and inelastic experimental cross sections involved.

In R-matrix scattering calculations employing a close-coupling expansion, all molecular target electronic states are represented by using a single set of molecular orbitals (MOs). This means that these MOs will not usually be optimal for a given target state. Indeed, the use of self-consistent field MOs for multistate calculations tends to overemphasize the ground state at the expense of excited states, leading to excitation energies that are too high. The choice of appropriate target MOs for use in a calculation can be difficult.[31] There are a number of possible choices of orbitals appropriate for representing several electronic states simultaneously. Up to now, there is no clear approach to choosing appropriate MOs, as discussed by Tennyson.[15] The target MO's representation generated from Multi-Configurational Self-Consistent Field (MCSCF) calculations is widely used. A common variant of the MCSCF method is the SA-CASSCF procedure, where all states for a given state-averaged active space, within which the electrons are freely distributed, are increasingly considered. However, there has been little exploration of the role of target MOs in obtaining high-accuracy collision results. In particular, the weights of electronic states in SA-CASSCF orbitals are usually determined automatically by the quantum chemistry package being used. A literature survey reveals only a few studies on this for electron-impact scattering by molecules. Harrison and Tennyson[32] make a rough estimate of electronic state weights, but no systematic evaluation has been conducted. Due to the complexity of scattering dynamics calculations, optimizing the target MOs using reliable experimental data, such as the dipole moment and molecular electronic energy, may improve both the accuracy and efficiency of the scattering calculations.

With this in mind, our primary goal is to develop an optimization framework capable of dealing with target MOs that allows one to reasonably model electron–molecule scattering processes subsequently. In this paper, we focus on the study of electron scattering

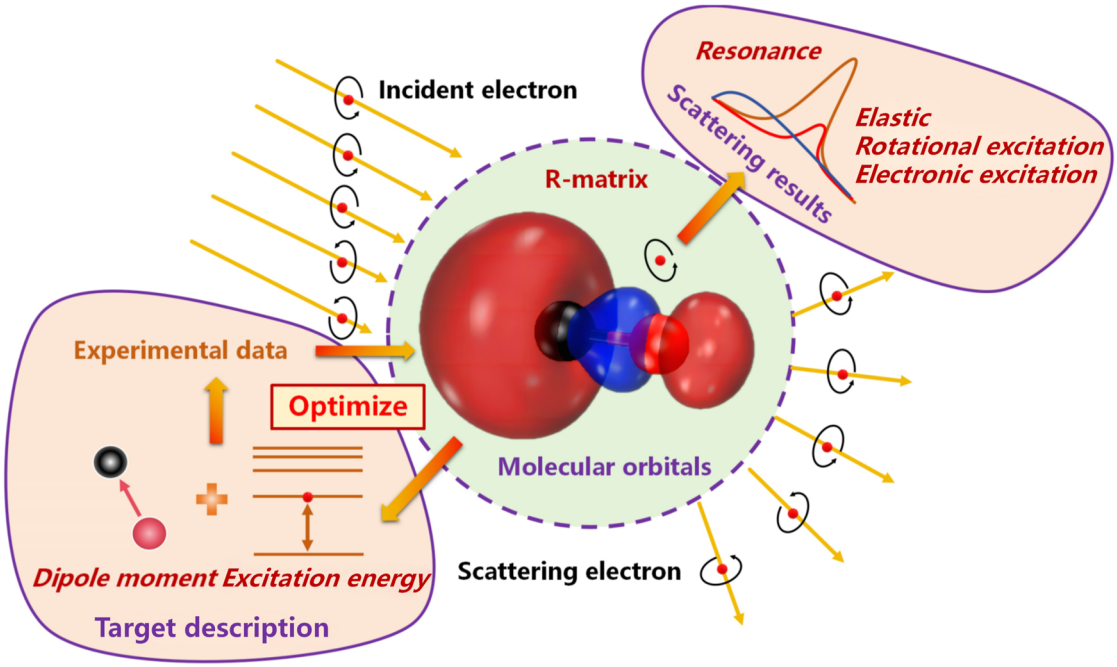

FIG. 1. Framework for electron–CO collision calculations with an optimization of target molecular orbitals used in the present study.

on carbon monoxide by using the R-matrix method with a CASSCF optimization of CO target MOs. This study can be described as shown in Fig. 1: first, we refine the number and weight of target electronic states for the description of target MOs automatically; using the optimized target MOs generated at different calculated levels, we then apply the R-matrix method to model electron-CO scattering processes; finally, we present a systemic analysis of elastic and inelastic cross sections along with the CO^- anion resonances.

II. METHODOLOGY

The accuracy of electron–molecule scattering calculation relies on an appropriate description of target wave functions. The SA-CASSCF method has been widely used to effectively generate target MOs in the subsequent low-energy electron–molecule scattering calculations using the R-matrix method.[33] A typical SA-CASSCF orbital is expressed as a linear combination of multiple molecular electronic states by the following form:

$$\Psi_{SA-CASSCF} = f_1\Psi_{orb1} + f_2\Psi_{orb2} + \cdots + f_n\Psi_{orbn}, \tag{1}$$

where Ψ_{orbi} represents the MOs of the ith target electronic state, f_i $(i = 1, 2, \ldots, n)$ is the corresponding weight, and n denotes the total number of the averaged target electronic states. The conventional optimal target MOs are obtained using the SA-CASSCF method by changing active spaces and/or increasing basis sets. However, it is insufficiently flexible to incorporate the needs of subsequent elastic and inelastic scattering processes. We note the factor f_i, which is typically left at its default value, merits further consideration. Here, we propose an automatic weighting optimization of target molecular wave functions based on reliable reference data, termed the optimization of target molecular orbitals (OTMOs) principle. Analogous to the weight optimization framework used in artificial neural networks,[34] we define an error function to quantify the discrepancy between predictions and experimental reference values,

$$\mathscr{L}(\boldsymbol{f}) = \sum_{t=1}^{n_{\text{state}}} \left[P_t^{\text{OTMO}}(f_1, f_2, \ldots, f_n) - P_t^{\text{ref}}\right]^2, \tag{2}$$

where n_{state} denotes the number of target electronic states included in the molecular representation, $P_t^{\text{OTMO}}(\boldsymbol{f})$ represents the optimized theoretical parameters as functions of the state weights, and P_t^{ref} corresponds to the experimentally derived reference values. The minimization of Eq. (2) employs a bifurcated optimization strategy, illustrated schematically in Fig. 2. The starting point is the implementation for the optimization with the number of target electronic states (step 1); then, we achieve the optimization according to the weight of each target state and select the optimal MOs (steps 2–5).

Numbering the target states provides an efficient protocol that expands the number of electronic states while maintaining equipartition $(f_i = n^{-1}, \forall i)$; the relevant low-lying excitations are prioritized, and the high-lying states are excluded. The optimal dimension n^* is determined as

$$\frac{\partial \mathscr{L}(n)}{\partial n} = 0 \quad \text{subject to} \quad f_i = \frac{1}{n},\ i = 1, 2, \ldots, n. \tag{3}$$

Step 2 involves weighting each target state. Utilizing the optimized target state number n^* obtained from the screening phase, we implement a cyclic coordinate descent algorithm[35] to refine the weight vector $\boldsymbol{f} = (f_1, f_2, \ldots, f_{n^*})$. The optimization equation is achieved by the following equation:

$$\sum_{i=1}^{n^*} \left|\frac{\partial \mathscr{L}(\boldsymbol{f})}{\partial f_i}\right| = 0. \tag{4}$$

Then, the ith parameter in the $(k+1)-$th iteration can be determined by the following equation:

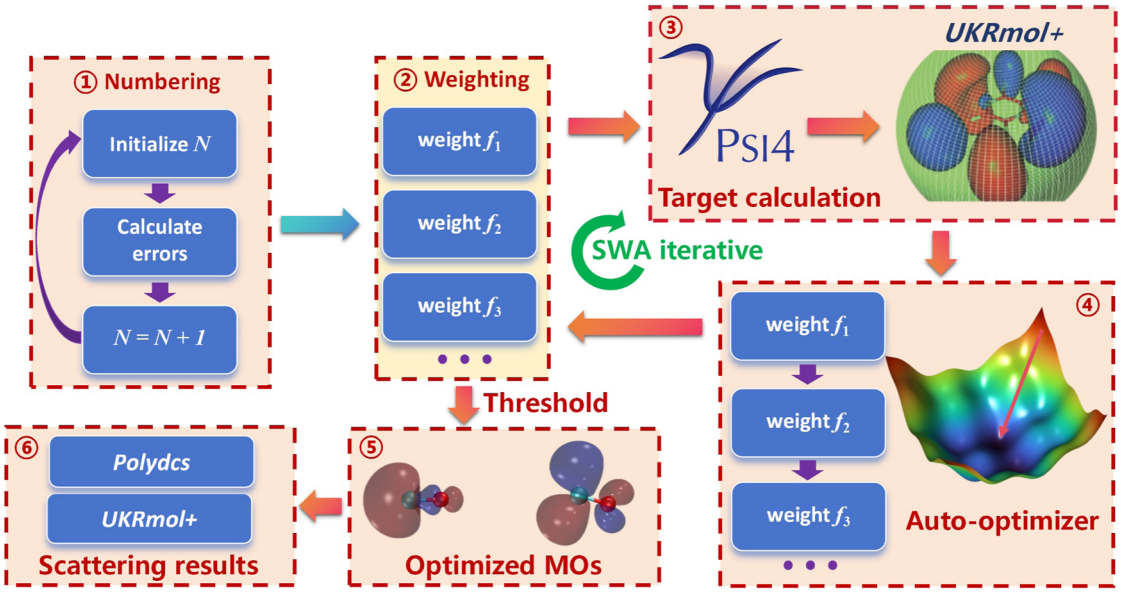

FIG. 2. Workflow for optimizing target molecular models and electron–molecule scattering calculations.

$$f_i^{(k+1)} = \arg\min_{f_i} \mathscr{L}(f_1^{(k+1)}, \ldots, f_{i-1}^{(k+1)}, f_i, f_{i+1}^{(k)}, \ldots, f_{n^*}^{(k)}). \quad (5)$$

Convergence is attained when successive iterations satisfy the termination criterion as below:

$$\left|\mathscr{L}(\boldsymbol{f}^{(N)}) - \mathscr{L}(\boldsymbol{f}^{(N-1)})\right| \le T_{\mathrm{tol}}, \quad (6)$$

where N denotes the final iteration index and T_{tol} represents the predefined tolerance threshold. The procedure generates a set of optimized MOs as displayed in Fig. 3.

Here, we apply our scheme to the modeling of electron–CO scattering. For reasons of computation resources and completeness of the continuum basis, we performed two sets of CASSCF calculations with a cc-pVTZ basis set for the optimization of target MOs. In both calculation sets, the lowest 1σ and 2σ core orbitals were kept frozen; the remaining ten electrons were allowed to occupy either eight or ten active orbitals, giving orbitals denoted hereafter as CAS_8 and CAS_{10}, respectively. Given that different physical processes of electron–CO molecule collisions may require distinct orbital information, here we employ a dual-optimization strategy: the MOs description is independently optimized using the electric dipole moment, which is important for elastic scattering, and by the electronic excitation energy with several target excited states, key for inelastic excitation processes. The optimized MOs can be defined as State Weighted Average with Dipole (SWAD) and State Weighted Average with Energy (SWAE) to denote their distinct optimization MOs in the OTMO framework.

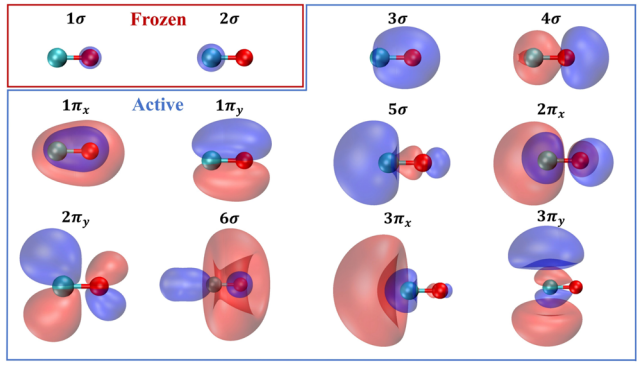

FIG. 3. Optimized CO target molecular orbitals employed in this study.

Table I summarizes the optimized parameters involving electronic excitation energies for the lowest seven electronic states and

TABLE I. CO ground target energies (in Hartree), vertical excitation energies, and their *RMSE* (in eV) for the lowest seven excited states compared to the adiabatic experimental values, and the ground state dipole moment (μ in Debye).

Method	$X\,^1\Sigma^+$	$a\,^3\Pi$	$a'\,^3\Sigma^+$	$A\,^1\Pi$	$d\,^3\Delta$	$e\,^3\Sigma^-$	$I\,^1\Sigma^-$	$D\,^1\Delta$	*RMSE*	μ
SWAD-CAS_{10}	−112.8962	6.39	8.97	9.59	9.84	10.22	10.56	10.60	0.58	0.150
SWAE-CAS_{10}	−112.8470	6.20	8.51	8.62	9.36	9.72	10.11	10.14	0.13	0.399
SWAD-CAS_8	−112.8406	6.14	8.44	8.92	9.22	9.54	9.89	9.88	0.26	0.116
SWAE-CAS_8	−112.8443	6.23	8.44	8.97	9.27	9.63	9.99	10.01	0.23	0.274
SA-CASCCF[21]	−112.8554	6.49	8.69	9.12	9.62	10.00	10.37	10.41	0.34	0.514
SA-CASCCF[23]	−112.8560	6.43	8.36	8.97	9.22	9.60	9.95	10.00	0.24	0.238
Experiment[36]		6.32	8.51	8.51	9.36	9.88	9.88	10.23		0.112

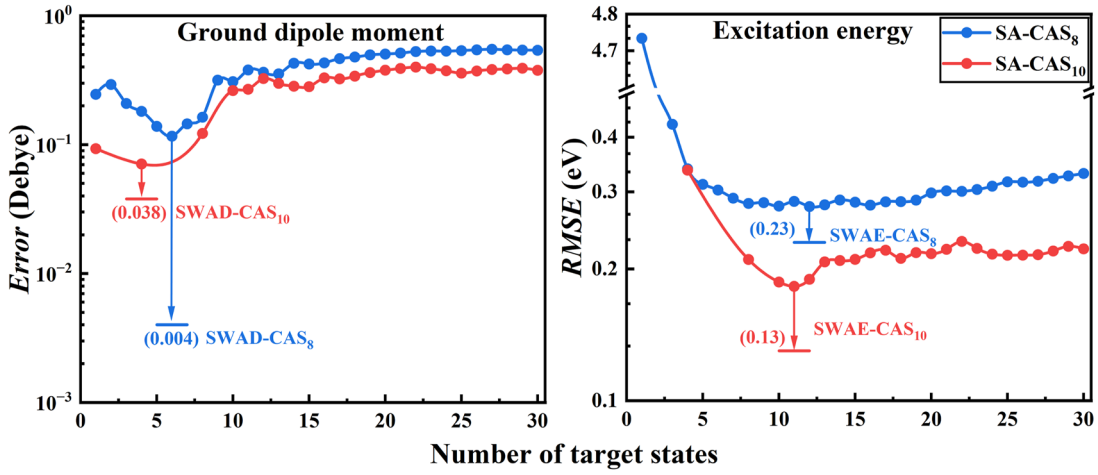

FIG. 4. *RMSE* of the electronic excitation energy (left) and the errors in the dipole moment (right) for the CAS_8 and CAS_{10} models.

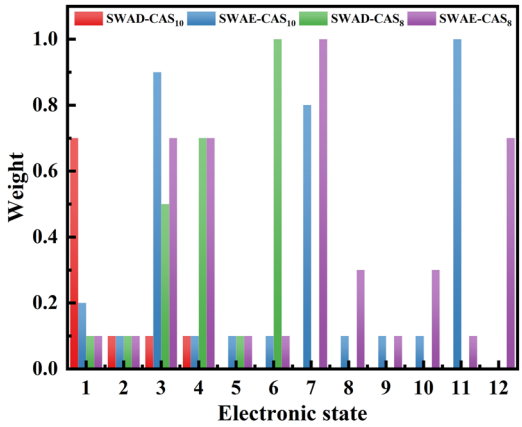

FIG. 5. Optimized weights for each CO target electronic state ordered by energy.

dipole moments for the CO target molecule with an equilibrium structure of 1.1282 Å. Figure 4 compares the absolute errors for the dipole moment and root-mean-square error (*RMSE*) for electronic excitation energies with the experimental data. The detailed number of coupled target states was also shown for each level. Figure 5 displays the optimized weight for each target state at various calculated levels. Considering the optimization of the number of target states, the state averaged SA − CAS_{10} calculations generally give lower *RMSE* than those of SA − CAS_8 in Fig. 4. Combining Table I with Fig. 4 (right), the improvements of the CO target description are demonstrated by comparing the lowest seven electronic excitation energies to the experiments within an *RMSE* of only 0.13 eV at the SAWE-CAS_{10} level, indicating the possibility of a high-accuracy description of the electron-impact excitation process.

The permanent dipole moment is important for dipole-induced transitions in the rotational excitation process. The best theoretical estimate of the CO equilibrium dipole moment is 0.1236(3) D[3]. The smallest error in the calculated dipole moment is 0.006 D, given by the SWAD-CAS_8 level calculation.

The optimal target MOs generated from the Psi4[37] package are used as input information for the subsequent electron-impact scattering calculations, which are performed by the UKRmol+[38] and POLYDCS[39] codes. The modeling of the low-energy electron scattering in polar molecules is typically carried out based on the *ab initio* R-matrix approach.[15] In the framework of the R-matrix approach, the configuration space for electron–molecule scattering can be divided into inner and outer regions by a sphere of radius $r = 10a_0$, centered on the molecular center of mass. Within this sphere, complex electron–molecule interactions involving electron exchange and polarization effects are treated explicitly, whereas the outer region only considers the long-range potential interactions with the scattering electron. In the inner region, the scattering electron is accurately modeled using a configuration interaction basis expansion for the total wave function, which can be expressed as

$$\Psi_k^{N+1}(x_1,\ldots,x_{N+1}) = \mathscr{A}\sum_{ij} a_{ijk}\Phi_i^N(x_1\ldots x_N)u_{ij}(x_{N+1}) + \sum_i b_{ik}\chi_i^{N+1}(x_1\ldots x_{N+1}), \quad (7)$$

where $\mathscr{A}$ is an antisymmetrization operator that accounts for the exchange between the target electrons and the scattering electron. The variational coefficients a_{ijk} and b_{ik} are determined by matrix diagonalization.[40] Φ_i^N is the wave function of the ith target state, and χ_i^{N+1} is the multicenter square-integrable L^2 correlation function. The u_{ij} represent the continuum orbitals of the scattering electron, for which Gaussian type orbitals[41] with partial waves with $l \le 6$ were used in this study. The scattering wave function in the inner region is represented by a close-coupling expansion involving 24 target states. The energy dependent scattering problem is solved by constructing R-matrices at distance $r = a$ from the center-of-mass, which are then propagated to asymptotic distances and matched with asymptotic solutions yielding K-matrices, which contain all the required information on the scattering process. Eigenphases, obtained from the K-matrix, are used to determine positions and widths of resonances. The transition T-matrices can be obtained from the K-matrix using the relation below:

$$\mathrm{T} = \frac{2i\mathrm{K}}{1 - i\mathrm{K}}. \quad (8)$$

which are then used to compute the state-to-state scattering cross section,

$$\sigma(i \to i') = \frac{\pi}{k_i^2}\sum_S \frac{(2S+1)}{2(2S_i+1)}\sum_{\Gamma ll'}\left|T^{\Gamma S}_{ili'l'}\right|^2, \quad (9)$$

where k_i is the wavenumber of the incident electron, S_i is the spin for the initial state, S is the spin of the total collision system, Γ represents the spatial symmetry representation, and l, l' are donated as the initial/final angular momentum quantum numbers. The dipole potential in molecules such as CO couples channels with $\Delta l = \pm 1$, requiring a partial-wave expansion to high l. The higher partial waves ($l > 6$) are included in scattering T-matrices via analytic Born T-matrices to ensure the effect of rotation involved; a similar approach[42] was used to Born-correct the electronic excitation cross sections considered here, which are both dipole-allowed.

III. ELECTRON–CO SCATTERING

Electron scattering events can be classified as either elastic or inelastic. In inelastic scattering, energy is exchanged between the projectile and the target, resulting in energy loss by the incident particle. Conversely, elastic scattering occurs without energy loss to the incident electron. Elastically scattered electrons can change their direction without changing their wavenumber. In this section, we analyze the total cross sections (TCS), momentum transfer cross sections (MTCS), elastic differential cross sections (DCS), rotational excitation cross sections (RECS), and inelastic electronic excitation cross sections (EECS), as well as CO^- anion resonances for electron collisions with CO molecules using the R-matrix method with target MOs optimization at four levels.

Electronic resonances are metastable states that can decay by electron loss, often manifesting as an enhancement in the scattering cross section. Here, we consider three CO^- anion resonances at the equilibrium structure, namely the low-lying $^2\Pi$ shape resonance, a second with $^2\Pi$ symmetry, and 1 $^2\Sigma^+$ symmetry resonance. A shape resonance is formed by an electron attaching to a molecule in its ground electronic state, usually at incident electron energies

below the first target excited threshold energy. Above this energy, resonances usually have a core-excited or mixed-shape-core-excited character. A core-excited resonance is formed when the incoming electron excites the target molecule to an electronically excited state (parent state), and simultaneously it is temporarily trapped in one of the unoccupied spin-orbitals. Feshbach resonances are core-excited resonances that lie below their parent target state; they generally have longer lifetimes than core-excited shape resonances. Therefore, the 1 $^2\Sigma^+$ resonant state with a very narrow resonance width suggests that it can reasonably be classified as a Feshbach resonance. The 2 $^2\Pi$ is located at around 10 eV, belonging to the core-excited resonant state. Dissociative electron attachment experiments suggest that there are resonances located between 10 and 11 eV,[43] corresponding to our 2 $^2\Pi$ and 1 $^2\Sigma^+$ resonances.

Resonance parameters were obtained by automatically fitting the eigenphases to a Breit–Wigner form.[44] Both 1 $^2\Pi$ and 2 $^2\Pi$ resonances are identified in all our calculations. Compared with the experimental result[45] of the 1 $^2\Pi$ state, our resonance positions and widths perform better than those of the previous R-matrix results using the large cc-pV6Z basis set.[23] In particular, our resonance position and width errors are only 0.006 and 0.07 eV, respectively, at the SWAE-CAS$_8$ level.

The scattering electron is temporarily trapped in the target potential well to enhance scattering cross sections. The TCS in Fig. 6 and the MTCS in Fig. 7 show that there is a pronounced peak located at around 2 eV, which is attributed to the formation of a typical 1 $^2\Pi$ shape resonance as shown in Table II, and the peak positions match the shape resonance energies very well at each level. Another weak hump is perceptible between 9 and 10 eV, which is associated with the 2 $^2\Pi$ and 1 $^2\Sigma^+$ resonance symmetries detected above. The pronounced rise in the TCS and MTCS as the incident energy decreases below 0.2 eV is due to the dipole moment of CO. In addition, the discrepancies between our results and the experiments may be attributed to uncertainties in the experimental reference values at very low energies.

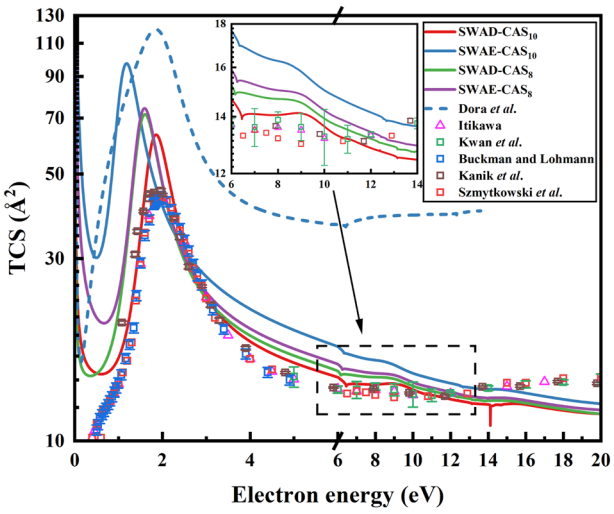

FIG. 6. Total cross sections for the CO molecule with optimized target molecular orbitals at SWAD and SWAE levels, in comparison to the previous R-matrix results of Dora and Tennyson.[22] The points represent the recommended data from Itikawa[14] and the experimental values of Kwan *et al.*,[4] Buckman and Lohmann,[5] Kanik *et al.*,[6] and Szmytkowski *et al.*[7]

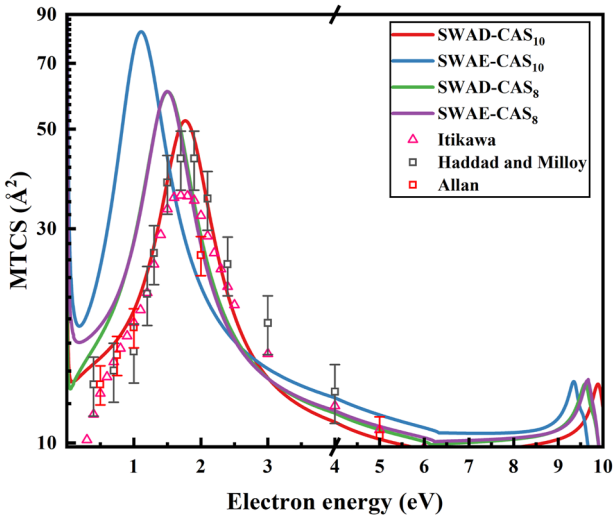

FIG. 7. Momentum transfer cross sections for the CO molecule with target molecular orbitals optimized at SWAD and SWAE levels, compared to the recommended data from Itikawa[14] and the experiments of Haddad and Millory,[11] as well as Allan.[12]

TABLE II. CO$^-$ anion resonance positions (and widths) at the equilibrium geometry; all quantities are in eV.

	1 $^2\Pi$	2 $^2\Pi$	1 $^2\Sigma^+$
SWAD-CAS$_{10}$	1.7677(0.7429)	11.2404(1.1364)	
SWAE-CAS$_{10}$	1.0897(0.6553)	10.5907(1.4974)	10.7129(0.0002)
SWAD-CAS$_8$	1.1511(0.7236)	10.7858(1.1952)	10.7542(0.0006)
SWAE-CAS$_8$	1.5064(0.6827)	10.8856(1.1878)	
SA-CASSCF[21]	1.73(0.84)		12.8999(0.0005)
SA-CASSCF[23]	1.8744(1.2916)		10.1019(0.1126)
Experiment[45]	1.50(0.75)		

The TCS and MTCS optimized at the SWAD-CAS$_{10}$ calculated level, involving only four target states as shown in Fig. 4 (right), prominently improve the accuracy, especially in the energy region up to 10 eV. The difference between SWAD-CAS$_{10}$ and SWAE-CAS$_{10}$ calculations is obvious. The results in the SWAE-CAS$_{10}$ calculations show higher peaks and lower positions than those of SWAD-CAS$_{10}$ orbitals, meaning that the use of the optimization from dipole moment provides a better treatment of correlation effects in both the target and anionic wave functions than those of excitation energies in the very low-energy regions. It is also worth noting that the elastic scattering processes are less sensitive to the details of the large number of target electronic states involved in MO optimization. In addition, our TCS from the target optimization with SWAD and SWAE are closer to the recommended values[14] and the experimental results[4–7] than the Born-corrected results using the

R-matrix method with the high-level cc-pV6Z basis set.[22] The crossing points between our TCS calculations and the experiments occur in the range of 8–12 eV; above that, the present optimized results are lower than those of the experiments, almost certainly due to the necessarily incomplete set of excited target electronic states that become open in this region. The TCS is dominated by electronic impact ionization at energies above the ionization threshold for CO, which is 14.01 eV;[46] this process is not considered in the present study.

Figure 8 shows a two-dimensional elastic DCS distribution for electron collisions with CO in the energy range up to 10 eV. It clearly shows that there are two distinct peaks separately at around 2 and 10 eV, which are mainly attributed to the formation of the three $1\ ^2\Pi$, $2\ ^2\Pi$, and $1\ ^2\Sigma^+$ resonances shown in Table II. Combining Figs. 8 and 9, we note that the DCS distributions tend to be flat between 3 and 9 eV. Overall, our DCS results compare very well with the previous experimental results of Gibson *et al.*[8] In particular, our elastic DCS below 5 eV at the SWAD-CAS$_{10}$ level is obviously closer to experiments than those of Gibson *et al.*[8] using the normal R-matrix method, indicating the prominent improvement in elastic DCS from the optimization of SWAD orbitals in the low-energy regions.

In the past, it was difficult to give high-accuracy DCS at low energies with narrow scattering angles in the R-matrix calculations. This is partly due to the domination of scattering processes by the dipole moment of a polar molecule at low incident energies and scattering angles,[47] as we discussed previously for pyridine.[48] Nevertheless, the DCS results below 2 eV using the optimized SWAD-CAS$_{10}$ give excellent agreement with experiment,[8] confirming that the state-weighting optimization of the dipole moment can provide reliable results. From 2.5 to 7.5 eV, our four types of calculations nearly overlap. Our results at the SWAE-CAS$_{10}$ level perform better than other calculations at 9.9 eV, presumably due to the complex electronic transition processes happening at this energy. Table I

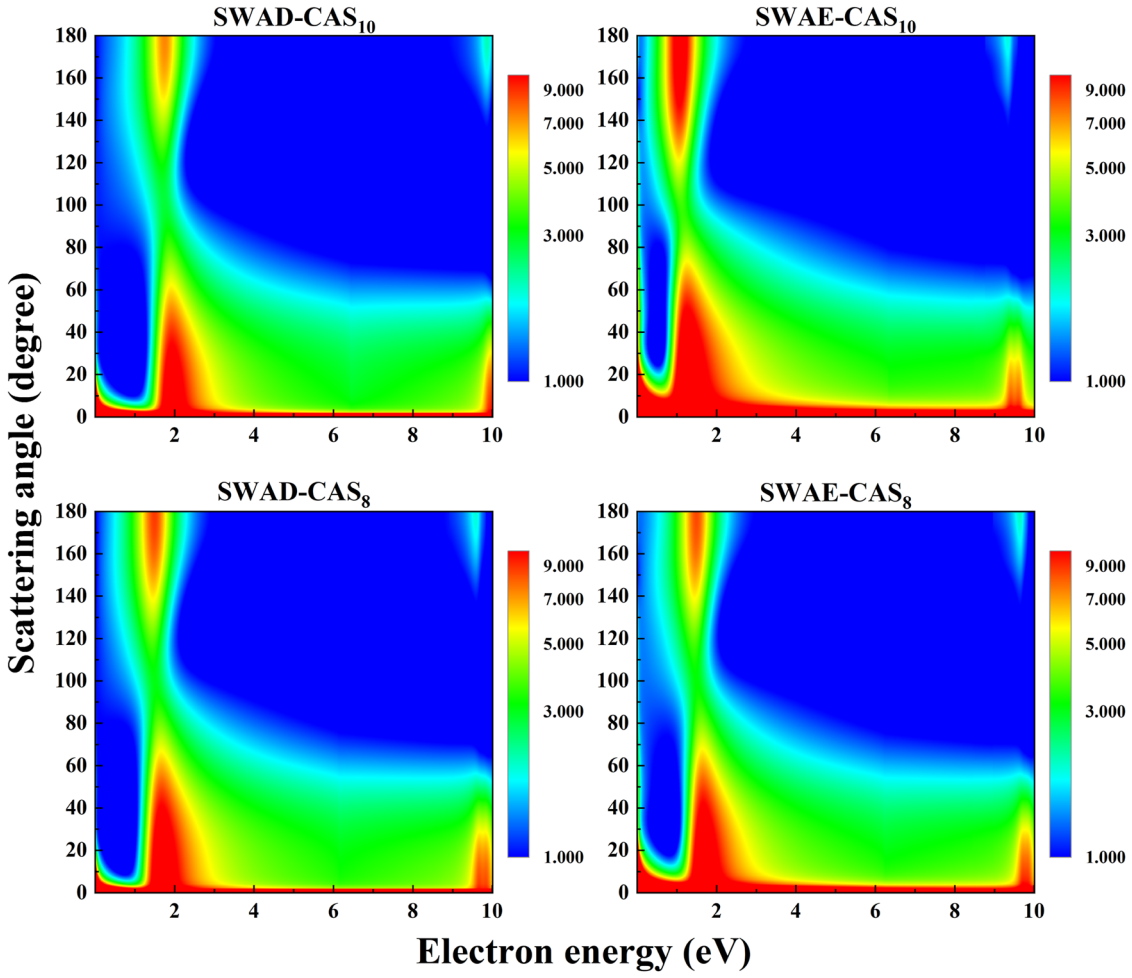

FIG. 8. Energy-dependent differential cross sections for elastic electron collisions with CO.

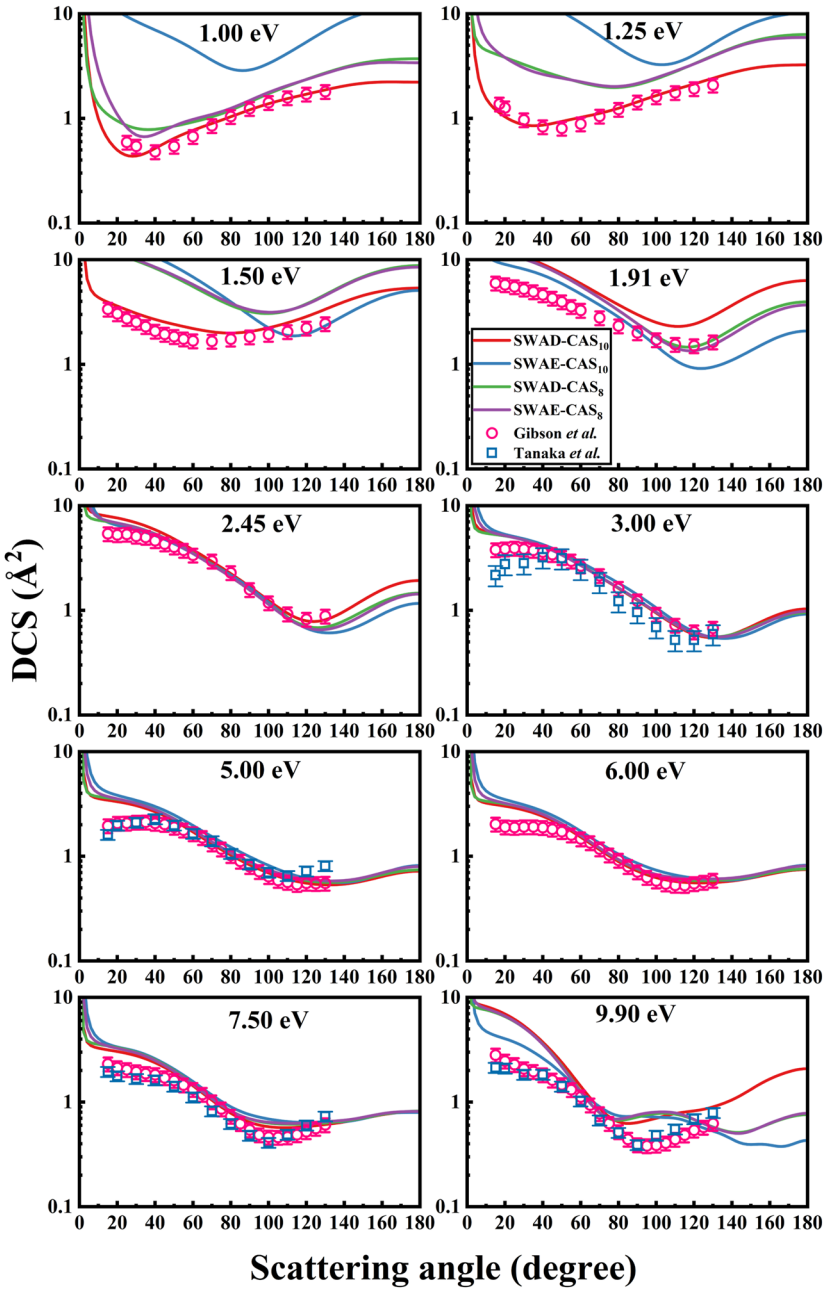

FIG. 9. Elastic differential cross sections for incident energies of 1, 1.25, 1.5, 1.91, 2.45, 3, 5, 6, 7.5, and 9.9 eV, comparisons of the experimental data of Gibson *et al.*[8] and Tanaka *et al.*[9]

shows that there are at least four CO excited states in the 9–10 eV range that can be reached by electron impact excitation; these states can be associated with the 2 $^2\Pi$ and 1 $^2\Sigma^+$ resonance states located at around 10 eV.

Accurate rotational excitation cross sections are difficult to measure and to estimate for molecules with a small permanent dipole moment like CO. State-to-state CO rotational cross sections from its rotational ground $j = 0$ state are presented for incident energies up to 10 eV. There are two distinct peaks located at around 2 and 10 eV in Fig. 10, that correspond to the three 1 $^2\Pi$, 2 $^2\Pi$, and 1 $^2\Sigma^+$ resonance states. The most likely process is pure elastic scattering to the $j' = 0$ state. The pure elastic cross section is found to be more than one order of magnitude higher than those for excitation to the $j' = 4$ and 5 rotational states, a process that is driven primarily by short-range interactions. It also shows that the dipole moment-induced transition to $j' = 1$ is the most likely excitation process. Moreover, our SWAD-CAS$_8$ optimized results are closer to the measurements[28] than previous R-matrix

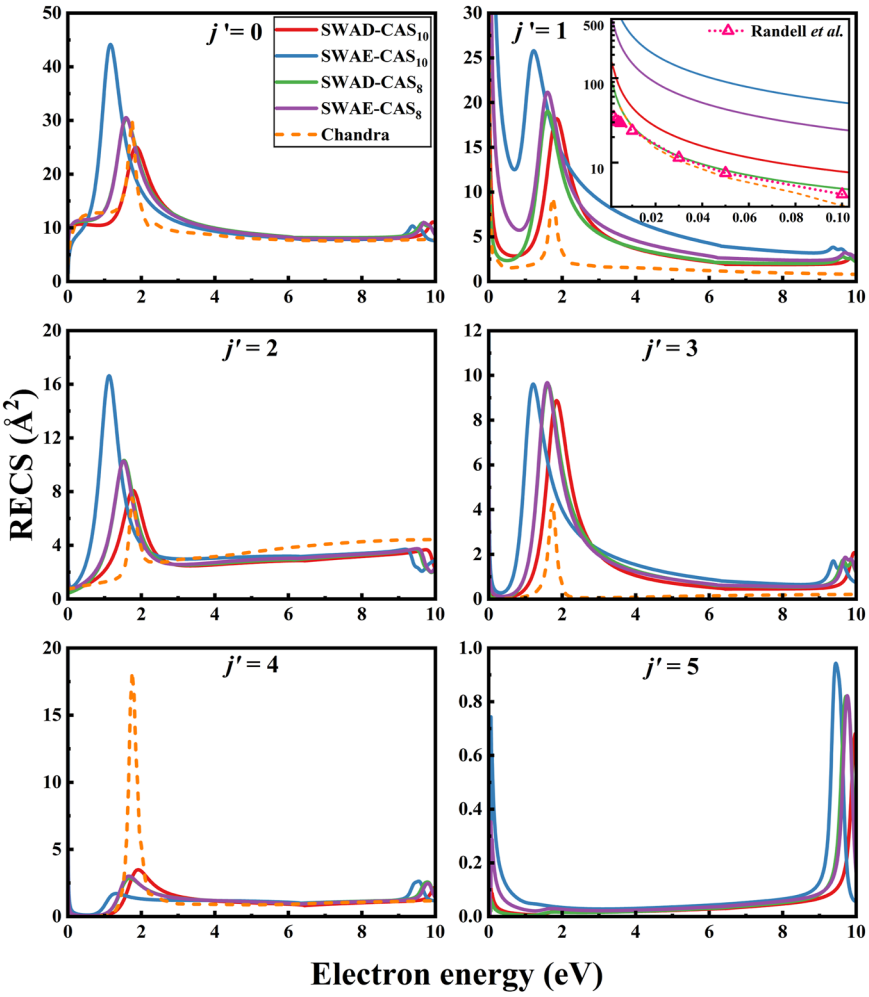

FIG. 10. Rotational excitation cross sections ($j = 0 \rightarrow j'$, $j' = 0, 1, 2, 3, 4, 5$) for CO with molecular orbitals optimized at the SWAD and SWAE levels, compared to the Wigner–Eisenbud R-matrix calculations from Chandra[27] and the measurements from Randell *et al.*[28]

calculations[27] at very low energies (below 0.1 eV). Our best dipole moment is provided by this model (see Table I), which is in line with the general expectation that rotational excitation transitions are generally dominated by dipole interactions. In addition, the rotational transition cross sections given by the SWAD-CAS_8 and SWAE-CAS_8 calculations almost overlap, except for excitation to $j' = 1$, which is possibly due to Born corrections used for this process.

The analysis of the inelastic excitation cross sections can not only provide additional electronic information for the CO molecule but also show different levels of performance and potential from our results. Figure 11 presents the EECS for electronic transitions from the ground $X\ ^1\Sigma^+$ to seven electronic excited states. The $2\ ^2\Pi$ and $1\ ^2\Sigma^+$ resonances in Table II reasonably account for the dominant peaks located at around 10 eV for the electronic excitation curves of $a\ ^3\Pi$ and $a'\ ^3\Sigma^+$. The EECS scattering results from the SWAD and SWAE generally align well with the recommended data.[14] A better agreement has been found between the present theoretical results and the measurements of Zawadzki *et al.*[24] when their experimental error becomes lower in the energy range for the first three excited states. In addition, our very low-scale EECS (below 0.05 Å^2) of the $I\ ^1\Sigma^-$ excited state matches the experiments[10] very well, meaning that our optimization calculations can accurately resolve the inelastic scattering process. It seems that our EECS of $a'\ ^3\Sigma^+$ exhibit a slightly different trend from the reference. Indeed, once we adjust for the excitation energy (a lowering of 1 eV, dashed line), the scattering results are in good agreement with the recommended data of Itikawa.[14] We note that the difference between the adiabatic and vertical excitation energies of $a'\ ^3\Sigma^+$ excited state is prominent, as shown in the CO potential energy curves (see Ref. 49); therefore, the better agreement obtained by shifting the excitation threshold is a reasonable approach in a fixed-nuclei calculation.

In terms of the EECS for the $a\ ^3\Pi$, $a'\ ^3\Sigma^+$, $A\ ^1\Pi$, and $I\ ^1\Sigma^-$ electronic excited states, Fig. 12 presents the *RMSE* compared to the recommended data of Itikawa[14] at four levels with different target

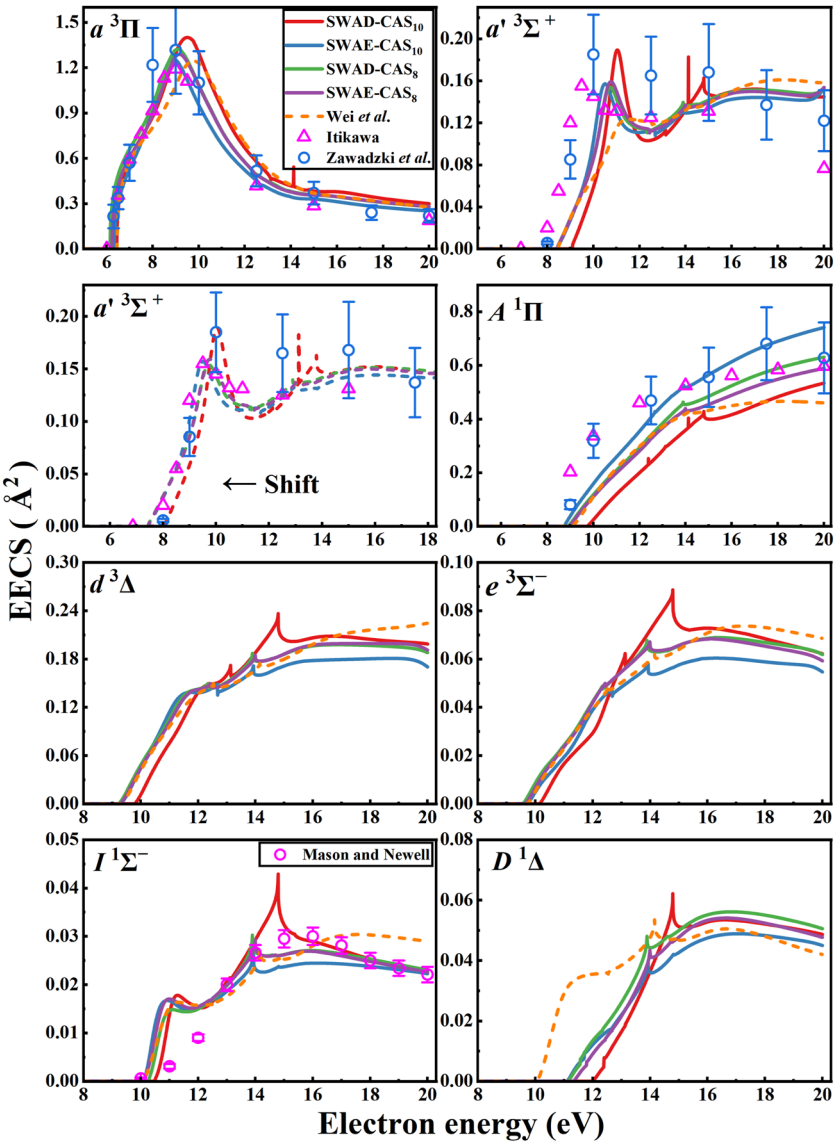

FIG. 11. Electronic excitation cross sections of CO from the $X\ ^1\Sigma^+$ ground state optimized at the SWAD and SWAE levels, compared to the previous R-matrix calculations from Wei *et al.*,[26] the recommended data from Itikawa,[14] and the measurements of Zawadzki *et al.*,[24] as well as Mason and Newell.[10] The dashed lines for the $a'\ ^3\Sigma^+$ state represent the results with a horizontal left shift of 1 eV at each optimized level.

optimizations. The SWAE-CAS_{10} calculations show the best performance with the lowest *RMSE* with a mere 0.06 $Å^2$. In comparison, we can also see that the trends between the *RMSE* of EECS and the *RMSE* of excitation energy are generally consistent. Therefore, we can conclude that the accurate description of target excitation energies is necessary in the modeling of inelastic scattering processes.

The SWAD-CAS_8 and SWAE-CAS_8 calculations nearly overlap over the whole energy region for both elastic and inelastic scattering processes, possibly due to reaching the upper limit of MO optimization for the low active space of CAS_8. Finally, above 13 eV spikes are observed in the cross section; these likely originate from pseudo-resonances, which are a known feature of close-coupling calculations at high energies. These spikes become more

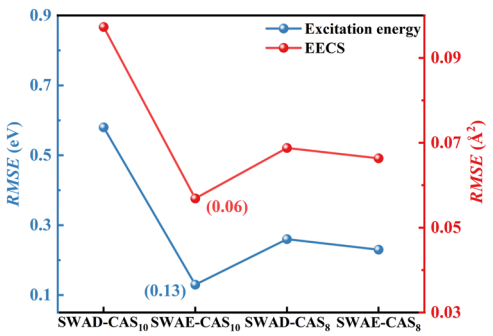

FIG. 12. *RMSE* of target vertical excitation energy and electronic excitation cross section separately at four optimized levels.

pronounced in calculations with large active spaces or high partial waves.

IV. CONCLUSIONS

In conclusion, we achieve unprecedented access to reasonable optimization of the CO target molecular orbitals, finding that the theoretical results of electron scattering with the optimized target CO molecule using the R-matrix method are in good agreement with available reference data in the low-energy region. Its key feature is an automated, data-driven optimization of the state-averaging weights in the SA-CASSCF calculations, which identify the optimal state-specific weights by minimizing the error function through an efficient dual-phase optimization framework. A good quality configuration interaction calculation is performed for the CO electronic ground and excited states. The improvements of the CO target description have been demonstrated by comparing the first seven electronic excitation energies to experiments within the lowest root-mean-square-error of 0.13 eV and the dipole moment error within only 0.006 D.

A systematic analysis of the cross sections as well as anion resonances for electron collisions with the CO molecule is presented. The dipole interactions dominate the elastic electron scattering process. It is found that the accuracy of the description of the target molecular dipole moment obviously affects the magnitude of elastic cross sections in the energy up to 10 eV, especially near the first $1\ ^2\Pi$ shaped resonance peak positions. The state weighted average with dipoles calculations give an excellent description of the elastic electron scattering process. The elastic differential cross sections, particularly below 5 eV with narrow scattering angles, from the optimization of SWAD-CAS_{10} perform in excellent agreement with the experiments, confirming that the state-weighting optimization of dipole moment can reasonably provide reliable results. The rotational excitation transition is significantly dominated by dipole interactions. The accurate target excitation energies play a key role in determining the inelastic electronic excitation scattering results. The weighted average with energy calculations performs excellently in the electronic excitation cross sections, even for the low-scale $I^1\Sigma^-$ excited states. The SWAE-CAS_{10} calculations show the best performance with a root-mean-square error with a mere 0.06 $Å^2$. The three CO^- anion resonant states involving one shape $1\ ^2\Pi$, one Feshbach $2\ ^2\Pi$, and one core-excited $1\ ^2\Sigma^+$ symmetry obviously enhance the cross sections.

From the results mentioned earlier, we conclude that our SWAD performs best for elastic and rotationally inelastic cross sections, while the SWAE model gives the best results for electronic excitation cross sections. This finding is consistent with the optimization approach adopted for each model. The present results provide a new insight that will aid in improving electron–molecule scattering in the low energy regions, and hopefully it can be extended to deal with other scattering events and complex molecules, since its central feature is the ability to calculate accurate molecular electronic wave functions appropriate for different processes.

ACKNOWLEDGMENTS

We acknowledge the support from the National Key R & D Program of China (Grant No. 2017YFA0303600), NSFC (Grant No. 11974253), Sichuan Science and Technology Program (Grant No. 2024ZYD0167), and the Natural Science Foundation of Sichuan Province (Grant No. 2022NSFSC1857).

AUTHOR DECLARATIONS

Conflict of Interest

The authors have no conflicts to disclose.

Author Contributions

Fan Fang: Conceptualization (equal); Data curation (lead); Formal analysis (equal); Investigation (equal); Methodology (equal); Software (equal); Writing – original draft (lead); Writing – review & editing (equal). **He Su**: Conceptualization (equal); Formal analysis (lead); Funding acquisition (equal); Investigation (lead); Resources (lead); Software (equal); Supervision (lead); Writing – review & editing (lead). **Jonathan Tennyson**: Formal analysis (equal); Investigation (equal); Methodology (equal); Software (equal); Supervision (equal); Writing – review & editing (equal). **Qunchao Fan**: Formal analysis (equal); Funding acquisition (equal); Resources (equal); Visualization (equal). **Zhixiang Fan**: Funding acquisition (equal); Investigation (equal); Resources (equal); Writing – original draft (equal). **Hong Zhang**: Investigation (equal); Resources (equal); Software (equal); Supervision (equal). **Xinlu Cheng**: Formal analysis (equal); Resources (equal); Supervision (equal); Writing – review & editing (equal).

DATA AVAILABILITY

The data that support the findings of this study are available from the corresponding author upon reasonable request.

REFERENCES

[1] K. Bartschat and M. J. Kushner, "Electron collisions with atoms, ions, molecules, and surfaces: Fundamental science empowering advances in technology," Proc. Natl. Acad. Sci. **113**, 7026–7034 (2016).
[2] J. Koput, "Toward accurate ab initio ground-state potential energy and electric dipole moment functions of carbon monoxide," J. Chem. Theor. Comput. **20**, 9041–9047 (2024).
[3] N. F. Zobov, R. I. Ovsyannikov, M. A. Rogov, E. I. Lebedev, J. Tennyson, and O. L. Polyansky, "CO line intensities: Towards subpercent accuracy of intensities of all bands," J. Quant. Spectrosc. Radiat. Transfer **345**, 109510 (2025).
[4] C. K. Kwan, Y. F. Hsieh, W. E. Kauppila, S. J. Smith, T. S. Stein, M. N. Uddin, and M. S. Dababneh, "e±−CO and e±−CO_2 total cross-section measurements," Phys. Rev. A **27**, 1328 (1983).
[5] S. J. Buckman and B. Lohmann, "Electron scattering from CO in the $^2\Pi$ resonance region," Phys. Rev. A **34**, 1561 (1986).
[6] I. Kanik, J. C. Nickel, and S. Trajmar, "Total electron scattering cross section measurements for Kr, $O_2$and CO," J. Phys. B Atom. Mol. Opt. Phys. **25**, 2189 (1992).
[7] C. Szmytkowski, K. Maciag, and G. Karwasz, "Absolute electron-scattering total cross section measurements for noble gas atoms and diatomic molecules," Phys. Scr. **54**, 271 (1996).
[8] J. C. Gibson, L. A. Morgan, R. J. Gulley, M. J. Brunger, C. T. Bundschu, and S. J. Buckman, "Low energy electron scattering from CO: Absolute cross section measurements and *R*-matrix calculations," J. Phys. B Atom. Mol. Opt. Phys. **29**, 3197 (1996).

[9]H. Tanaka, S. K. Srivastava, and A. Chutjian, "Absolute elastic differential electron scattering cross sections in the intermediate energy region. IV. CO," J. Chem. Phys. **69**, 5329–5333 (1978).
[10]N. J. Mason and W. R. Newell, "Electron impact excitation of a higher lying metastable state of carbon monoxide," J. Phys. B Atom. Mol. Opt. Phys. **21**, 1293 (1988).
[11]G. Haddad and H. Milloy, "Cross sections for electron-carbon monoxide collisions in the range 1–4 eV," Aust. J. Phys. **36**, 473–484 (1983).
[12]M. Allan, "Electron collisions with CO: Elastic and vibrational excitation cross sections," Phys. Rev. A **81**, 042706 (2010).
[13]M. J. Brunger and S. J. Buckman, "Electron–molecule scattering cross-sections. I. Experimental techniques and data for diatomic molecules," Phys. Rep. **357**, 215–458 (2002).
[14]Y. Itikawa, "Cross sections for electron collisions with carbon monoxide," J. Phys. Chem. Ref. Data **44**, 013105 (2015).
[15]J. Tennyson, "Electron–molecule collision calculations using the R-matrix method," Phys. Rep. **491**, 29–76 (2010).
[16]P. G. Burke, *R-matrix Theory of Atomic Collisions: Application to Atomic, Molecular and Optical Processes* (Springer Science & Business Media, 2011), Vol. 61.
[17]L. A. Morgan and J. Tennyson, "Electron impact excitation cross sections for CO," J. Phys. B Atom. Mol. Opt. Phys. **26**, 2429 (1993).
[18]J. Tennyson, "**R**-matrix calculation of Rydberg states of CO," J. Phys. B Atom. Mol. Opt. Phys. **29**, 6185–6201 (1996).
[19]V. Laporta, C. M. Cassidy, J. Tennyson, and R. Celiberto, "Electron-impact resonant vibration excitation cross sections and rate coefficients for carbon monoxide," Plasma Sources Sci. Technol. **21**, 045005 (2012).
[20]V. Laporta, J. Tennyson, and R. Celiberto, "Carbon monoxide dissociative attachment and resonant dissociation by electron-impact," Plasma Sources Sci. Technol. **25**, 01LT04 (2016).
[21]A. Dora, J. Tennyson, and K. Chakrabarti, "Higher lying resonances in low-energy electron scattering withcarbon monoxide," The Eur. Phys. J. D **70**, 197 (2016).
[22]A. Dora and J. Tennyson, "Electron collisions with CO molecule: An R-matrix study using a large basis set," in *Quantum Collisions and Confinement of Atomic and Molecular Species, and Photons* (Springer, 2019), pp. 48–59.
[23]A. Dora and J. Tennyson, "Electron collisions with CO molecule: Potential energy curves of higher lying CO^- resonant states," J. Phys. B Atom. Mol. Opt. Phys. **53**, 195202 (2020).
[24]M. Zawadzki, M. A. Khakoo, L. Voorneman, L. Ratkovich, Z. Mašín, K. Houfek, A. Dora, R. Laher, and J. Tennyson, "Low energy inelastic electron scattering from carbon monoxide: I. Excitation of the a3Π, a′ 3Σ+ and a1Π electronic states," J. Phys. B Atom. Mol. Opt. Phys. **53**, 165201 (2020).
[25]M. Zawadzki, M. A. Khakoo, A. Sakaamini, L. Voorneman, L. Ratkovich, Z. Mašín, A. Dora, R. Laher, and J. Tennyson, "Low energy inelastic electron scattering from carbon monoxide: Ii. Excitation of the $b^3\Sigma+$, $j^3\Sigma+$, $B^1\Sigma+$, $C^1\Sigma+$ and $E^1\Pi$ Rydberg electronic states," J. Phys. B Atom. Mol. Opt. Phys. **55**, 025201 (2022).
[26]P. Wei, C. Huang, X. Cheng, and H. Zhang, "Low-energy inelastic electron scattering from carbon monoxide: Excitation and de-excitation of the $X^1\Sigma+$, $a^3\Pi$, $a'^3\Sigma+$, $A^1\Pi$, $d^3\Delta$, $e^3\Sigma^-$, $I1\Sigma^-$ and $D^1\Delta$ electronic states," Chin. Phys. B **33**, 043101 (2024).
[27]N. Chandra, "Low-energy electron scattering from CO. II. *Ab initio* study using the frame-transformation theory," Phys. Rev. A **16**, 80 (1977).
[28]J. Randell, R. J. Gulley, S. L. Lunt, J.-P. Ziesel, and D. Field, "Very low energy electron scattering in CO," J. Phys. B Atom. Mol. Opt. Phys. **29**, 2049 (1996).
[29]M.-T. Lee, I. Iga, L. M. Brescansin, L. E. Machado, and F. B. C. Machado, "Theoretical studies on electron-carbon monoxide collisions in the low and intermediate energy range," J. Mol. Struct.: THEOCHEM **585**, 181–187 (2002).
[30]M. M. Billah, M. H. Khandker, M. Shorifuddoza, M. Sayed, H. Watabe, A. Haque, and M. A. Uddin, "Theoretical investigations of e±−CO scattering," J. Phys. B Atom. Mol. Opt. Phys. **54**, 095203 (2021).
[31]L. K. McKemmish, S. N. Yurchenko, and J. Tennyson, "*Ab initio* calculations to support accurate modelling of the rovibronic spectroscopy calculations of vanadium monoxide (VO)," Mol. Phys. **114**, 3232–3248 (2016).
[32]S. Harrison and J. Tennyson, "Electron collisions with the CN radical: Bound states and resonances," J. Phys. B Atom. Mol. Opt. Phys. **45**, 035204 (2012).
[33]K. Houfek, J. Benda, Z. Mašín, A. Harvey, T. Meltzer, V. Graves, and J. D. Gorfinkiel, "UKRmol-scripts: A perl-based system for the automated operation of the photoionization and electron/positron scattering suite UKRmol+," Comput. Phys. Commun. **298**, 109113 (2024).
[34]D. E. Rumelhart, G. E. Hinton, and R. J. Williams, "Learning representations by back-propagating errors," Nature **323**, 533–536 (1986).
[35]S. J. Wright, "Coordinate descent algorithms," Math. Program. **151**, 3–34 (2015).
[36]R. D. Johnson III, "NIST 101. Computational chemistry comparison and benchmark database," Computational Chemistry Comparison and Benchmark Database, http://cccbdb.nist.gov, 1999.
[37]J. M. Turney, A. C. Simmonett, R. M. Parrish, E. G. Hohenstein, F. A. Evangelista, J. T. Fermann, B. J. Mintz, L. A. Burns, J. J. Wilke, M. L. Abrams, N. J. Russ, M. L. Leininger, C. L. Janssen, E. T. Seidl, W. D. Allen, H. F. Schaefer, R. A. King, E. F. Valeev, C. D. Sherrill, and T. D. Crawford, "Psi4: An open-source *ab initio* electronic structure program," Wiley Interdiscip. Rev.: Comput. Mol. Sci. **2**, 556–565 (2011).
[38]Z. Mašín, J. Benda, J. D. Gorfinkiel, A. G. Harvey, and J. Tennyson, "UKRmol+: A suite for modelling electronic processes in molecules interacting with electrons, positrons and photons using the R-matrix method," Comput. Phys. Commun. **249**, 107092 (2020).
[39]N. Sanna and F. A. Gianturco, "Differential cross sections for electron/positron scattering from polyatomic molecules," Comput. Phys. Commun. **114**, 142–167 (1998).
[40]J. Tennyson, "A new algorithm for Hamiltonian matrix construction in electron - molecule collision calculations," J. Phys. B Atom. Mol. Opt. Phys. **29**, 1817–1828 (1996).
[41]A. Faure, J. D. Gorfinkiel, L. A. Morgan, and J. Tennyson, "GTOBAS: Fitting continuum functions with Gaussian-type orbitals," Comput. Phys. Commun. **144**, 224–241 (2002).
[42]S. Kaur, K. L. Baluja, and J. Tennyson, "Electron-impact study of NeF using the r-matrix method," Phys. Rev. A **77**, 032718 (2008).
[43]P. Nag and D. Nandi, "Fragmentation dynamics in dissociative electron attachment to CO probed by velocity slice imaging," Phys. Chem. Chem. Phys. **17**, 7130–7137 (2015).
[44]J. Tennyson and C. J. Noble, "RESON—A program for the detection and fitting of Breit-Wigner resonances," Comput. Phys. Commun. **33**, 421–424 (1984).
[45]M. Zubek and C. Szmytkowski, "Electron impact vibrational excitation of CO in the range 1–4 eV," Phys. Lett. **74**, 60–62 (1979).
[46]D. Rapp and P. Englander-Golden, "Total cross sections for ionization and attachment in gases by electron impact. I. Positive ionization," J. Chem. Phys. **43**, 1464–1479 (1965).
[47]R. Zhang, A. Faure, and J. Tennyson, "Electron and positron collisions with polar molecules: Studies with the benchmark water molecule," Phys. Scr. **80**, 015301 (2009).
[48]H. Su, X. Cheng, B. Cooper, J. Tennyson, and H. Zhang, "Elastic and inelastic low-energy electron scattering from pyridine," J. Chem. Phys. **158**, 024301 (2023).
[49]L. Peng-Fei, Y. Lei, Y. Zhong-Yuan, G. Yu-Feng, and G. Tao, "An accurate calculation of potential energy curves and transition dipole moment for low-lying electronic states of CO," Commun. Theor. Phys. **59**, 193 (2013).